

**Quantum Zeno and anti-Zeno effect of a nanomechanical resonator measured by a point contact**Po-Wen Chen,<sup>1,\*</sup> Dong-Bang Tsai,<sup>2</sup> and Philip Bennett<sup>3</sup><sup>1</sup>*Department of Physics, National Taiwan University, Taipei 10617, Taiwan*<sup>2</sup>*Research Center for Applied Sciences, Academia Sinica, Taipei 11529, Taiwan*<sup>3</sup>*Department of Education Portfolio, Meadowbank College, Sydney, Australia*

(Received 25 December 2008; revised manuscript received 18 January 2010; published 8 March 2010; corrected 2 April 2010)

The occurrence of either the quantum Zeno effect (QZE) or anti-Zeno effect (AZE) resulting from the short-time behavior of the environment-induced decoherence for quantum Brownian motion (QBM) model has been discussed [S. Maniscalco, J. Piilo, and K. A. Suominen, *Phys. Rev. Lett.* **97**, 130402 (2006)]. We discuss here while the shuttering time period (length) of the frequent observations is changed, the system of interest, i.e., a nanomechanical oscillator, will undergo a QZE to AZE crossover. Instead of interacting with an equilibrium bosonic bath in a QBM model, we investigate the occurrence of either QZE or AZE of a nanomechanical oscillator coupled to a nonequilibrium fermionic reservoir [quantum point contact (QPC) detector as a measuring device]. We find that Zeno and anti-Zeno behaviors depend on the values of the system and reservoir parameters such as the oscillator frequency, energy cutoff, bias voltage, and reservoir temperature.

DOI: [10.1103/PhysRevB.81.115307](https://doi.org/10.1103/PhysRevB.81.115307)

PACS number(s): 03.67.Mn, 03.65.Xp, 03.65.Yz

**I. INTRODUCTION**

The rapid development of nanotechnology in recent years has ushered in a new generation of quantum electronic devices incorporating the mechanical degrees of freedom, so-called nanoelectromechanical systems.<sup>1-5</sup> Recently, mechanical resonators with vibrational eigenfrequencies on the order of 1 GHz have been fabricated.<sup>6,7</sup> The standard cantilever displacement measurement schemes are based on laser interferometry, and can reach the levels of sensitivity on the order of  $10^{-4}$  Å/ $\sqrt{\text{Hz}}$ , opening new avenues of technology in high-precision quantum measurement. Quantum oscillations of nanomechanical resonators can provide an attractive platform for testing quantum phenomena at macroscopic scales. It has also been suggested<sup>8</sup> that gigahertz-frequency nanomechanical resonators can be used to coherently couple two or more Josephson junction qubit together to make a flexible and scalable solid-state quantum-information-processing architecture. This is why the problem of the decoherence and relaxation of a nanomechanical oscillator (continuous system), interacting with an environment or a measurement device, has become a very important issue in quantum computing and information.<sup>9-11</sup> In general, the influences of a surrounding environment or a detector on the nanomechanical oscillator system is of important for the sake of understanding oscillator measurements when the detector (environment) is acting on the oscillator in different decay regimes.<sup>9,12</sup> The key quantity in these discussions is the reduced density matrix  $\rho(t)$  of the nanomechanical oscillator defined as the partial trace of the total system-plus-reservoir density operator  $\rho_T(t)$  over the reservoir degrees of freedom; i.e.,  $\rho(t) = \text{Tr}_R[\rho_T(t)]$ . We investigate here in this paper, the occurrence of either quantum Zeno effect (QZE) or anti-Zeno effect of a nanomechanical oscillator coupled to a nonequilibrium fermionic reservoir (quantum point-contact detector) acting as a measuring device.

The quantum Zeno effect predicts that the decay of an unstable system can be slowed down by measuring the system frequently enough. On the other hand, the enhancement

of the decay due to frequent measurements may be called an anti-Zeno effect or inverse Zeno effect (AZE).<sup>13-15</sup> Recently, Maniscalco<sup>15</sup> *et al.* had investigated the Zeno-anti-Zeno crossover in quantum Brownian motion (QBM) model dealing with a system of damped harmonic oscillator interacting with a bosonic reservoir in thermal equilibrium. They demonstrate the short-time behavior of environment-induced decoherence due to the interaction between the system and its surroundings. The goal of that paper was to investigate the conditions for the occurrence of the quantum Zeno and anti-Zeno processes using the QBM model, for a damped harmonic oscillator under decoherence induced by a controlled environment. The use of artificially controllable engineered environments has already been demonstrated for single trapped ions.<sup>16,17</sup> The possibility of controlling both the environment and the system-environment couplings would allow one to monitor the transition from Zeno to anti-Zeno dynamics. In Ref. 18, it was proposed to use a single trapped ion coupled to engineered reservoirs in order to simulate quantum Brownian motion by applying noisy electric fields. Shuttering these noisy electric fields, one can model a fast switch off-on of the environment which implies that when the noise is off, the reservoir simply does not exist anymore. The action of the sudden switch off-on of the environment may be seen as a physical implementation of the operation of trace over the reservoir degrees of freedom. The operation of trace is a typical example of a nonselective measurement.<sup>9</sup> Hence, a succession of short switch off-on periods, realized by shuttering the engineered applied noise, would induce Zeno or anti-Zeno dynamics depending on the value of the system and reservoir parameters and of the shuttering period. This was the core idea for monitoring the Zeno-anti-Zeno crossover with trapped ions.

Quantum point contact (QPC) as a measurement device for nanomechanical oscillator is studied in the past although to the best of our knowledge there is no discussion on the Zeno-anti-Zeno condition in this literature for this system. In analogy with the study of Ref. 18, here in our case, one can do a fast switch off-on of the environment by controlling the shuttering time of the noisy electric field. When the noise is

switched off, the reservoir simply does not exist anymore. The action of switch off-on of the environment may be seen as a physical implementation of trace operation over the reservoir degrees of freedom. Our results show that making a fast switch off-on (successive switch on-off over a short-time period) realized by the engineered applied noise, one would induce Zeno or anti-Zeno dynamics. When the shuttering time period of the frequent observations is changed, the system of interest, i.e., a nanomechanical oscillator, will undergo a QZE to AZE crossover. Here we investigate the occurrence of either QZE or AZE of a nanomechanical oscillator coupled to a nonequilibrium fermionic reservoir (quantum point-contact detector acting as a measuring device).

In this paper, we focus on a nanomechanical oscillator coupled to a nonequilibrium fermionic reservoir to determine the occurrence of either the Zeno or the anti-Zeno effect due to the nonequilibrium fermionic-reservoir-induced decoherence. In our model, QPC detector will act as an engineered detector. One can switch on-off the electric bias across the QPC controlling the shuttering time of the effective environment. In Sec. II, we describe our model for a nanomechanical oscillator coupled to a nonequilibrium fermionic reservoir (a QPC acting as measuring device). We investigate the non-Markovian regime by taking into account the Fermi-reservoir correlation. The memory effect on the electron transport can be studied in detail by modeling the reservoir spectral densities as Lorentzian functions that has been used in the study of influence of a measuring lead on quantum oscillator coupled to an electron reservoirs.<sup>19–23</sup> We do not make here the so-called wideband approximation (energy-independent spectral density of the electric bath, and energy-independent tunnel amplitudes and densities of states of the left and right leads of the QPC tunnel junction) as well as the high QPC bias-voltage-limit approximation, normally used<sup>24,25</sup> in the derivation of Markovian dynamical equations. As a consequence, our non-Markovian dynamics of the nanomechanical oscillator is valid for arbitrary QPC lead temperatures, and for arbitrary bias voltages, as long as the perturbation theory that we use holding up to the second order in the system-environment coupling strength. In Sec. III, we demonstrate significant the results and discussions. Finally, Sec. IV contains some conclusions and remarks.

## II. MODEL

In this section, we describe the model of nanoelectromechanical resonator (NER) that is subjected to a measurement by a low-transparency point contact or electric tunneling junction as a sensitive detector device.<sup>5,25–29</sup> The Hamiltonian model consists of a quantum harmonic oscillator linearly coupled to a nonequilibrium fermionic reservoir<sup>25</sup> (a quantum point-contact detector as a measuring device) (Fig. 1) and derive their corresponding quantum master equations up to the second order with respect to the system-environment coupling constant. The Hamiltonian of the NER which is linearly coupled to the QPC can be written as

$$H = H_S + H_{leads} + H_T, \quad (1)$$

where

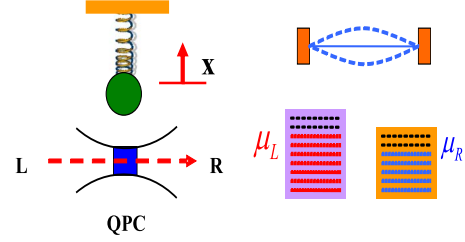


FIG. 1. (Color online) Schematic of a nanomechanical resonator measured by a quantum point contact (QPC).

$$H_S = \frac{p^2}{2M} + \frac{1}{2}M\omega_o^2x^2, \quad (2)$$

$$H_{leads} = \sum_{k,q} (\epsilon_k^S c_k^\dagger c_k + \epsilon_q^D c_q^\dagger c_q), \quad (3)$$

and

$$H_T = \sum_{k,q} (T_{k,q} + \chi_{kq}x) c_{S,k}^\dagger c_{D,q} + \sum_{k,q} (T_{k,q}^\dagger + \chi_{kq}^\dagger x) c_{D,q}^\dagger c_{S,k}. \quad (4)$$

$H_S$  represents the effective Hamiltonian for nanomechanical oscillator,  $M$  is the mass, and  $\omega_o$  is the frequency of oscillator, respectively. The Hamiltonian for the left and right leads of the QPC detector is represented by  $H_{leads}$ . Here  $c_{S,k}$ ,  $c_{D,q}$  and  $\epsilon_k^S$ ,  $\epsilon_q^D$  are, respectively, the fermion- (electron) reservoir annihilation operators and the energies with wave numbers  $k, q$  for the left and right leads of the QPC. In Eq. (4),  $H_T$  describes the tunneling of the electrons through the QPC junction under the influence of the displacement  $x$  of the NER. The bare tunneling amplitude between respective states  $k$  and  $q$  in the left and right leads (reservoirs) of the QPC is given by  $T_{k,q}$ . The effective tunneling amplitude<sup>27</sup> becomes  $T_{kq} + \chi_{kq}x$  as a result of the coupling Eq. (4) between the NER and QPC. We will derive the quantum master equation for the oscillator under Born approximation which holds up to second order in the effective tunneling amplitude. To proceed to the derivation, it is convenient to go to interaction picture with respect to  $H_0 = H_S + H_{leads}$ . The dynamics of the entire system is determined by the time-dependent Hamiltonian in interaction picture.<sup>9,30</sup> For convenience, we reexpress the tunneling Hamiltonian in the interaction picture as

$$\begin{aligned} H_I(t) &= e^{iH_0 t} H_T e^{-iH_0 t} \\ &= \sum_{k,q} [T_{kq} + \chi_{kq}x(t)] e^{i(\epsilon_k^S - \epsilon_q^D)t} c_{S,k}^\dagger c_{D,q} + \text{H.c.} \\ &= \sum_{k,q} [Q_{k,q}(t) F_{k,q}^\dagger(t) + Q_{k,q}^\dagger(t) F_{k,q}(t)], \end{aligned} \quad (5)$$

where  $Q_{k,q}(t) = [T_{kq} + \chi_{kq}x(t)]$  and  $F_{k,q}(t) = e^{-i(\epsilon_k^S - \epsilon_q^D)t} c_{S,k}^\dagger c_{D,q}$  are operators acting on the Hilbert space of the system and environment, respectively. Here  $x(t) = x \cos[\omega_o t] + \frac{p}{m\omega_o} \sin[\omega_o t] = (\frac{x}{2} - i\frac{p}{2m\omega_o}) \exp[i\omega_o t] + (\frac{x}{2} + i\frac{p}{2m\omega_o}) \exp[-i\omega_o t]$ . In Eq. (5), we reexpress the tunneling Hamiltonian as follows:

$$H_I(t) = \sum_{k,q} S_{kq}(t) F_{kq}^\dagger(t) + S_{kq}^\dagger(t) F_{kq}(t), \quad (6)$$

where

$$S_{kq}(t) = [P_1 + e^{i\hbar\omega_o t} P_2 + e^{-i\hbar\omega_o t} P_3] \quad (7)$$

is an operator in a discrete Fourier decomposition<sup>31</sup> acting on the Hilbert space of the system. Here  $P_1 = T_{kq}$ ,  $P_2 = \chi_{kq}(\frac{x}{2} - i\frac{p}{2m\omega_o})$ , and  $P_3 = \chi_{kq}(\frac{x}{2} + i\frac{p}{2m\omega_o})$ . The form indicates that, three possible jump processes,  $P_1$  is associated with elastic tunneling of electrons through QPC,  $P_2$  (and  $P_3$ ) are associated with inelastic excitation (and relaxation) of electrons tunneling through the QPC with an energy transfer  $\hbar\omega_o$ . This energy is provided by the oscillator which relaxes (excites) in response. By regarding the tunneling Hamiltonian as perturbation, the second-order cumulant expansion (Born approximation) leads to the master equation for the reduced density matrix of the NER system. We will derive non-Markovian master equation implemented with the memory kernel prescription.<sup>32</sup> By partially taking trace over the microscopic degrees of freedom of the QPC reservoir and then changing from the interaction picture to the Schrödinger picture, we obtain the non-Markovian master equation in the following form:

$$\begin{aligned} \dot{\rho}_R(t) &= \frac{1}{i\hbar} [H_S, \rho_R] - \frac{1}{\hbar^2} \int_0^t dt_1 \sum_{k,q;k',q'} \\ &\times \left[ F_{k,q;k',q'}^S(t, t_1) ([S_{k,q}, [S_{k',q'}^\dagger(t, t_1), \rho_R]] \right. \\ &\left. + F_{k,q;k',q'}^A(t, t_1) ([S_{k,q}, \{S_{k',q'}^\dagger(t, t_1), \rho_R\}] + \text{H.c.}] \right] \quad (8) \end{aligned}$$

where the mode-dependent symmetric and antisymmetric two-time correlation function,  $F_{k,q;k',q'}^S(t, t_1)$  and  $F_{k,q;k',q'}^A(t, t_1)$  can be written in term of the new variable  $\tau (= t - t_1)$  as

$$\begin{aligned} F_{k,q;k',q'}^S(t, t_1) &= F_{k,q;k',q'}^S(\tau, 0) \\ &= \frac{1}{2} \langle \{F_{k,q}^\dagger(\tau), F_{k',q'}(0)\} \rangle \\ &= \frac{1}{2} \langle (c_{S,k}^\dagger c_{D,q} c_{D,q'}^\dagger c_{S,k'} + c_{D,q'}^\dagger c_{S,k'} c_{S,k}^\dagger c_{D,q}) e^{i(\epsilon_k^S - \epsilon_q^D)\tau} \rangle \\ &\equiv \frac{1}{2} \langle \{N_{Sk}(1 - N_{Dq}) + (1 - N_{Sk})N_{Sk}\} e^{i(\epsilon_k^S - \epsilon_q^D)\tau} \delta_{k,q;k',q'} \rangle \quad (9) \end{aligned}$$

and

$$\begin{aligned} F_{k,q;k',q'}^A(t, t_1) &= F_{k,q;k',q'}^A(\tau, 0) \\ &= \frac{1}{2} \langle [F_{k,q}^\dagger(\tau), F_{k',q'}(0)] \rangle \\ &= \frac{1}{2} \langle (c_{S,k}^\dagger c_{D,q} c_{D,q'}^\dagger c_{S,k'} - c_{D,q'}^\dagger c_{S,k'} c_{S,k}^\dagger c_{D,q}) e^{i(\epsilon_k^S - \epsilon_q^D)\tau} \rangle \\ &\equiv \frac{1}{2} \langle \{N_{Sk}(1 - N_{Dq}) - (1 - N_{Sk})N_{Sk}\} e^{i(\epsilon_k^S - \epsilon_q^D)\tau} \delta_{k,q;k',q'} \rangle \quad (10) \end{aligned}$$

We have transformed the temporal integrals into integrals over variable  $\tau = t - t_1$ . Here the bracket notations  $F_{k,q;k',q'}^S(\tau, 0)$  [and  $F_{k,q;k',q'}^A(\tau, 0)$ ] indicate the symmetric (and antisymmetric) combinations of the distribution function determined by the two-time correlation function of Fermi environment. The occupation number of Fermi function is,  $N_{Sk} = \langle c_{S,k}^\dagger c_{S,k} \rangle \delta_{kk'}$ , where  $\langle \dots \rangle$  stands for the statistical average over the Fermi distribution for left and right electron reservoirs given by  $N_{Sk} = [e^{\beta(\epsilon_k^S - \mu_k)} + 1]^{-1}$  and  $N_{Dq} = [e^{\beta(\epsilon_q^D - \mu_D)} + 1]^{-1}$ .<sup>33,34</sup> We have used here the basic unraveling schemes, for controlling of continuous variable system.<sup>27</sup> Here  $\rho_R$  is the reduce density matrix,  $\rho_R = \text{Tr}_{S,D}[\rho_R \otimes \rho_B^{(0)}]$ , where  $\rho_B^{(0)} = \rho_S \otimes \rho_D = \exp(-\frac{H_{\text{QPC}}}{k_B T}) / \text{Tr}_R[\exp(-\frac{H_{\text{QPC}}}{k_B T})]$ . Here  $\mu_S$  and  $\mu_D$  are the chemical potentials of the source and the drain reservoir which determine the applied detector voltage,  $\mu_S - \mu_D = eV$ , and  $\beta = 1/(k_B T)$  is the inverse temperature.<sup>33,34</sup>

The structure of the quantum point-contact reservoir is characterized by the symmetric and antisymmetric two-time reservoir correlation kernels  $\sum_{k,q;k',q'} W_{kq}^\dagger Z_{kq} F_{k,q;k',q'}^S(t, t_1)$  and  $\sum_{k,q;k',q'} W_{kq}^\dagger Z_{kq} F_{k,q;k',q'}^A(t, t_1)$ , where  $W_{kq}$  and  $Z_{kq}$  can be any one of the tunneling amplitudes  $T_{kq}$  or  $\chi_{kq}$ . In the continuous limit, the summation of reservoir modes can be replaced by the continuous integrations,  $\sum_{k,q} \rightarrow \iint d\epsilon_k^S d\epsilon_q^D g_L(\epsilon_k) g_R(\epsilon_q)$ , where the energy-dependent densities of states  $g_S(\epsilon_k)$ ,  $g_D(\epsilon_q)$  are introduced for left and right electron reservoirs.<sup>33</sup> In principle, the tunneling amplitudes,  $T_{kq}(\epsilon_k^S, \epsilon_q^D)$  and  $\chi_{kq}(\epsilon_k^S, \epsilon_q^D)$ , are also energy dependent. We may deal with relevant energy function of form the densities of states and tunneling amplitudes to take into account the memory effect of the QPC reservoir on the electron transport and the NER system in non-Markovian treatment. For simplicity, we follow several non-Markovian electron-transport studies<sup>19-21,23,35</sup> and we consider a Lorentzian spectral density with energy-dependent density of states and tunneling amplitudes as

$$\begin{aligned} J_{W,Z}(\epsilon_k^S, \epsilon_q^D) &= W_{kq}^\dagger(\epsilon_k^S, \epsilon_q^D) Z_{kq}(\epsilon_k^S, \epsilon_q^D) g_L(\epsilon_k^S) g_R(\epsilon_q^D) \\ &\simeq \frac{W_{00}^\dagger Z_{00}^0 g_L^0 g_R^0(\lambda)^2}{(|\epsilon_k^S - \epsilon_q^D - E_i|)^2 + (\lambda)^2} \quad (11) \end{aligned}$$

Here  $W_{kq}(\epsilon_k^S, \epsilon_q^D)$  and  $Z_{kq}(\epsilon_k^S, \epsilon_q^D)$  could be any one of the tunneling amplitudes,  $T_{kq}$  or  $\chi_{kq}$ , the cutoff energy  $\lambda$  describes the width of the Lorentzian energy-dependent distribution, the parameter  $E_i$  denotes the variation in the QPC

junction barrier potential due to the interaction with the NER. The energy dependence of the tunneling amplitudes and the density of states are absorbed into the combined form of the denominator of the spectral density, and  $W_{00}$ ,  $Z_{00}$ ,  $g_L^0$ , and  $g_R^0$  are energy-independent tunneling amplitudes and densities of states near the average chemical potential. In the limit of  $\lambda \rightarrow 0$  and in absence of the interaction with the NER (i.e.,  $E_j=0$ ), the QPC spectral density Eq. (11) is proportional to  $\delta(\epsilon_k^S - \epsilon_q^D)$  which represents the resonant tunneling process. In the opposite case of the cutoff energy  $\lambda \rightarrow \infty$ , the QPC spectral density Eq. (11) becomes energy independent and reduces to the wideband limit (WBL) which spectral density is recovered with a constant. The average (effective) electron-tunneling rates through the QPC barrier in the WBL can be written as  $\Gamma = 2\pi W_{00}^\dagger Z_{00} g_L^0 g_R^0$ .

Meier *et al.*<sup>36</sup> had investigated expression for bath correlation via the technique of numerical decomposition of the spectral density and rederived auxiliary density matrices to be able to describe memory effects. The spectral decomposition technique has been used for non-Markovian dissipative system<sup>21</sup> with a Lorentzian spectral density to calculate the fermionic-reservoir correlation function. The spectral density function is a very important in decomposition technique which can handle an arbitrary band structure using the parameter  $\lambda$ .<sup>37</sup> The width of the Lorentzian distribution is characterized by the cutoff parameter  $\lambda$ . The non-Markovian memory effect arises due to a finite cutoff width of the spectral density function.

With the help of Eqs. (9) and (10) and using the specified spectral density [Eq. (11)], we can rewrite the master Eq. (8) into the following form:

$$\begin{aligned} \dot{\rho}_R(t) = & -\frac{i}{\hbar}[H_S, \rho_R(t)] \\ & -\frac{2g_L^0 g_R^0}{\hbar^2} \left\{ \sum_{j=1}^3 [f_F^\dagger(t, eV + \hbar\omega_j) + f_B^\dagger(t, -eV - \hbar\omega_j)] \right. \\ & \times [PP_j^\dagger \rho_R(t) - P_j^\dagger \rho_R(t)P + P\rho_R(t)P_j^\dagger + \rho_R(t)P_j^\dagger P] \\ & - \sum_{j=1}^3 [f_F^\dagger(t, eV + \hbar\omega_j) - f_B^\dagger(t, -eV - \hbar\omega_j)] \\ & \left. \times [PP_j^\dagger \rho_R(t) - P_j^\dagger \rho_R(t)P + P\rho_R(t)P_j^\dagger + \rho_R(t)P_j^\dagger P] \right\} \\ & + \text{H.c.} \end{aligned} \quad (12)$$

Here  $P_1 = T_{00}$ ,  $P_2 = \chi_{00}(\frac{x}{2} - i\frac{p}{2m\omega_0})$ , and  $P_3 = \chi_{00}(\frac{x}{2} + i\frac{p}{2m\omega_0})$ ,  $P = \sum_{j=1}^3 P_j = P_1 + P_2 + P_3$ , and the frequencies  $\omega_1 = 0$  and  $\omega_2 = -\omega_3 = \omega_0$ . Thus the time-dependent coefficients in the second to the fifth lines of Eq. (12) describe the forward and backward electron tunneling in elastic (no excitation of the NER) or inelastic (excitation or relaxation of the NER) processes. We have introduced here some new notations  $\omega_k^S = \epsilon_k^S - \mu_k$  and  $\omega_q^D = \epsilon_q^D - \mu_q$ . Here the time-dependent coefficients of the forward (backward) tunneling rates in elastic process,  $f_F^\dagger(t, eV)$  [ $f_B^\dagger(t, -eV)$ ] are given by

$$\begin{aligned} f_F^\dagger(t, eV) \equiv & \int_0^t d\tau \int_{-\infty}^{\infty} \int_{-\infty}^{\infty} d\omega_k^S d\omega_q^D \frac{\lambda^2}{(|\epsilon_k - \epsilon_q - E_i|)^2 + \lambda^2} \\ & \times \frac{1}{e^{\beta\omega_k^S} + 1} \left( 1 - \frac{1}{e^{\beta\omega_q^D} + 1} \right) e^{\pm i(\omega_k^S - \omega_q^D - eV)\tau} \\ = & \text{Re}[f(t, eV)] \pm i \text{Im}[f(t, eV)] \end{aligned} \quad (13)$$

and

$$\begin{aligned} f_B^\dagger(t, -eV) \equiv & \int_0^t d\tau \int_{-\infty}^{\infty} \int_{-\infty}^{\infty} d\omega_k^S d\omega_q^D \frac{\lambda^2}{(|\epsilon_k - \epsilon_q - E_i|)^2 + \lambda^2} \\ & \times \left( 1 - \frac{1}{e^{\beta\omega_k^S} + 1} \right) \frac{1}{e^{\beta\omega_q^D} + 1} e^{\pm i(\omega_k^S - \omega_q^D - eV)\tau} \\ = & \text{Re}[f(t, -eV)] \pm i \text{Im}[f(t, -eV)]. \end{aligned} \quad (14)$$

On the other hand, time-dependent coefficients of the forward (backward) tunneling rates in inelastic process  $f_F^\dagger(t, eV \pm \hbar\omega_0)$  [ $f_B^\dagger(t, -eV \mp \hbar\omega_0)$ ] are given by

$$\begin{aligned} f_F^\dagger(t, eV \pm \hbar\omega_0) \equiv & \int_0^t d\tau \int_{-\infty}^{\infty} \int_{-\infty}^{\infty} d\omega_k^S d\omega_q^D \\ & \times \frac{\lambda^2}{(|\epsilon_k - \epsilon_q - E_i|)^2 + \lambda^2} \frac{1}{e^{\beta\omega_k^S} + 1} \\ & \times \left( 1 - \frac{1}{e^{\beta\omega_q^D} + 1} \right) e^{\pm i(\omega_k^S - \omega_q^D - eV \pm \hbar\omega_0)\tau} \\ = & \text{Re}[f(t, eV \pm \hbar\omega_0)] \pm i \text{Im}[f(t, eV \pm \hbar\omega_0)] \end{aligned} \quad (15)$$

and

$$\begin{aligned} f_B^\dagger(t, -eV \pm \hbar\omega_0) \equiv & \int_0^t d\tau \int_{-\infty}^{\infty} \int_{-\infty}^{\infty} d\omega_k^S d\omega_q^D \\ & \times \frac{\lambda^2}{(|\epsilon_k - \epsilon_q - E_i|)^2 + \lambda^2} \frac{1}{e^{\beta\omega_q^D} + 1} \\ & \times \left( 1 - \frac{1}{e^{\beta\omega_k^S} + 1} \right) e^{\pm i(\omega_k^S - \omega_q^D - eV \pm \hbar\omega_0)\tau} \\ = & \text{Re}[f(t, -eV \pm \hbar\omega_0)] \\ & \pm i \text{Im}[f(t, -eV \pm \hbar\omega_0)]. \end{aligned} \quad (16)$$

The non-Markovian environmental memory effect is characterized by the forward and backward correlation functions  $f_F^\dagger(t, eV)$ ,  $f_B^\dagger(t, -eV)$ ,  $f_F^\dagger(t, eV \mp \hbar\omega_0)$ , and  $f_B^\dagger(t, -eV \mp \hbar\omega_0)$ . Non-Markovian dynamics usually means past history that contributes to the current time evolution and memory effects typically enter through integrals over the past history. Within the second-order perturbation theory in the system-detector and system-environment coupling strengths, the non-Markovian dynamics is determined by the state at the current time  $t$  only.<sup>38,39</sup> Finally, the non-Markovian master equation for the nanomechanical oscillator coupled to a electric tunneling junction Eq. (12) reduces to a form similar to the Markovian Caldeira-Leggett-type master equation<sup>26,27,40</sup> as

$$\begin{aligned} \dot{\rho}_R(t) = & -\frac{i}{\hbar} \left[ H_S + \frac{M}{2} [\omega_e^2(t)] x^2, \rho_R(t) \right] - \frac{i}{\hbar} \gamma_e(t) [x, \{\rho_R(t)\}] \\ & - \frac{1}{\hbar^2} D_e(t) [x, [x, \rho_R(t)]] + \frac{1}{\hbar^2} h_e(t) [x, [p, \rho_R(t)]]. \end{aligned} \quad (17)$$

The whole non-Markovian character of nanomechanical oscillator is contained in the time-dependent coefficients appearing in the master equation. The time-dependent coefficients  $\omega_e^2(t)$ ,  $\gamma_e(t)$ ,  $D_e(t)$ , and  $h_e(t)$  are respectively given by

$$\omega_e^2(t) = \frac{\alpha}{\pi M} \text{Im}[\xi_2^a(t) + \xi_1^a(t)], \quad (18)$$

$$\gamma_e(t) = \frac{\alpha}{2\pi M \omega_o} \text{Re}[\xi_1^s(t) - \xi_2^s(t)], \quad (19)$$

$$D_e(t) = \frac{\hbar \alpha}{2\pi} \text{Re}[\xi_1^s(t) + \xi_2^s(t)], \quad (20)$$

$$h_e(t) = \frac{\hbar \alpha}{2\pi M \omega_o} \text{Im}[\xi_1^s(t) - \xi_2^s(t)]. \quad (21)$$

Where  $\alpha = \frac{2\pi}{\hbar} g_L^0 g_R^0 \lambda^2$ ,  $\xi_1^s(t) = f(t, eV + \hbar\omega_o) + f(t, -eV - \hbar\omega_o)$ ,  $\xi_1^a(t) = f(t, eV + \hbar\omega_o) - f(t, -eV - \hbar\omega_o)$ ,  $\xi_2^s(t) = f(t, eV - \hbar\omega_o) + f(t, -eV + \hbar\omega_o)$ , and  $\xi_2^a(t) = f(t, eV - \hbar\omega_o) - f(t, -eV + \hbar\omega_o)$ . The time-dependent coefficients in Eqs. (18)–(21) are composed of forward and backward tunneling rates containing the electron bath temperature, electric voltage, and the oscillator frequency. The coefficient  $\omega_e^2(t)$  leads to a time-dependent energy shift.<sup>41</sup> The second and third terms on the right-hand side in Eq. (17) represent physically the influences of friction and fluctuations of the environment. The damping coefficient  $\gamma_e(t)$  and diffusion coefficient  $D_e(t)$  are determined by the real part of the reservoir QPC correlation functions. On the other hand, the time-dependent coefficient  $h_e(t)$  is determined by the imaginary part of the QPC reservoir correlation function. We can calculate explicitly all the time-dependent non-Markovian transport coefficients and compare with their Markovian counterpart in various time scales. The time-dependent coefficients of the diffusion and damping terms  $D_e(t)$  and  $\gamma_e(t)$  are plotted in Figs. 2(a) and 2(b) with different finite Lorentzian cutoff strengths ( $\lambda$ ) in the non-Markovian region. The coefficients  $D_e(t)$  and  $\gamma_e(t)$  are plotted in Figs. 2(c) and 2(d) for different electric bias voltage in the non-Markovian region. We see (Fig. 2) that the non-Markovian time-dependent coefficients  $D_e(t)$  and  $\gamma_e(t)$  approach to the Markovian value at large time as one increases the cutoff frequency  $\lambda$ . Under this wideband ( $\lambda \rightarrow \infty$ ) and long-time limit, our non-Markovian master equation reduces to Caldeira-Leggett-type Markovian master equation as discussed in Refs. 27 and 40. We have explicitly shown this in Appendix. In the Markovian case (when the bath correlation time is shorter than the system response time), we assume that the bath correlation function is delta function. Under those two limit, the Markovian coefficients are given by

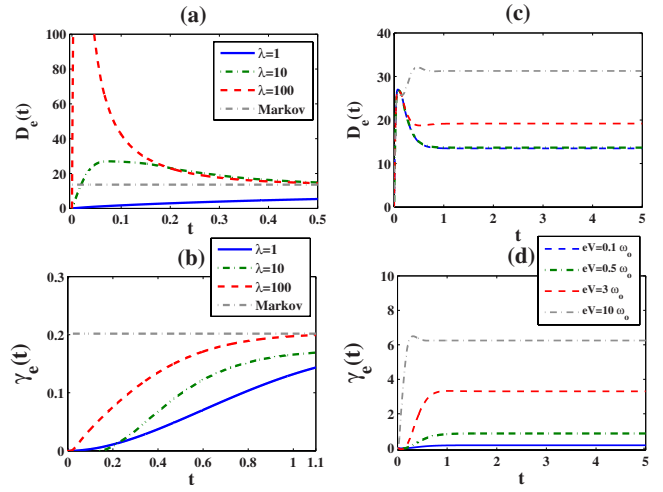


FIG. 2. (Color online) The time-dependent coefficients  $D_e(t)$  and  $\gamma_e(t)$  for the non-Markovian case are plotted against time in Figs. 2(a) and 2(b) with different Lorentzian cutoff strengths  $\lambda$  (from top to bottom  $\lambda=1, 10, 100, \infty$ ). The value of the other parameters for Figs. 2(a) and 2(b) are  $eV=0.1\omega_o$ ;  $\beta=10\omega_o$ . The coefficients  $D_e(t)$  and  $\gamma_e(t)$  for the non-Markovian case are plotted in Figs. 2(c) and 2(d) with different electric bias voltage  $eV$  (from top to bottom  $eV=0.1\omega_o, 0.5\omega_o, 3\omega_o, 10\omega_o$ ). The value of the other parameters for Figs. 2(c) and 2(d) are  $\beta=10\omega_o$ ,  $\lambda=10$ .

$$\gamma_e^M = \lim_{\lambda, t \rightarrow \infty} \gamma_e(t) = \frac{2\pi g_L^0 g_R^0 \lambda^2}{M} = \frac{\hbar}{M} \alpha \quad (22)$$

and

$$\begin{aligned} D_e^M &= \lim_{\lambda, t \rightarrow \infty} D_e(t) \\ &= \frac{\hbar \alpha}{2} \left[ (eV + \hbar\omega_o) \coth \frac{eV + \hbar\omega_o}{2k_B T} \right. \\ &\quad \left. + (eV - \hbar\omega_o) \coth \frac{eV - \hbar\omega_o}{2k_B T} \right] \\ &= \frac{M \gamma_e^M}{2} \left[ (eV + \hbar\omega_o) \coth \frac{eV + \hbar\omega_o}{2k_B T} \right. \\ &\quad \left. + (eV - \hbar\omega_o) \coth \frac{eV - \hbar\omega_o}{2k_B T} \right]. \end{aligned} \quad (23)$$

In the non-Markovian case,  $D_e(t)$  and  $\gamma_e(t)$  depend on electric bias voltage, electric reservoir temperature, and oscillator frequency. But in the Markovian limit, the coefficient  $D_e^M$  depends upon those parameters.<sup>27</sup> The phenomenological parameters  $D_e^M$  and  $\gamma_e^M$  are related to each other by the fluctuation-dissipation theorem. In the special case of zero temperature and high-voltage case, we simply have  $D_e^M = \hbar \gamma_e^M eV$  which is exactly the same result that was obtained in Refs. 25–27. Also, in the high-temperature limit<sup>42</sup> when  $k_B T \gg eV$  or  $\hbar\omega_o$ , the diffusion coefficient  $D_e^M = 2\hbar \gamma_e^M k_B T$ . It is clear from Fig. 2 that the non-Markovian dynamics is quite different in general from the Markovian case.

Next we discuss our main results indicate that the occurrence of the Zeno or the anti-Zeno effect stems from the short-time behavior of the Fermi-reservoir-induced decoherence showing the Zeno-anti-Zeno crossover.

### III. RESULT AND DISCUSSION

The time-dependent coefficients appearing in Eq. (17) contain all the information about the short-time system-reservoir correlation. Consequently, each switching off and on process will reset the correlations between the system and the environment. The use of artificial controllable engineered environments has been recently demonstrated for single trapped ions.<sup>17</sup> Averaging over the rapidly oscillating terms appearing in the time-dependent coefficients of Eq. (17), one gets the following secular approximation in Refs. 13 and 43 of master equation, by means of rotating wave approximations performed after tracing over the environment in Eq. (17),<sup>13,44</sup>

$$\begin{aligned} \dot{\rho}_R(t) = & -\frac{i}{\hbar}[H_S, \rho_R(t)] \\ & + \frac{D_e(t) + \gamma_e(t)}{2}[2a\rho_R(t)a^\dagger - a^\dagger a\rho_R(t) - \rho_R(t)a^\dagger a] \\ & + \frac{D_e(t) - \gamma_e(t)}{2}[2a^\dagger \rho_R(t)a - aa^\dagger \rho_R(t) - \rho_R(t)aa^\dagger], \end{aligned} \quad (24)$$

where we have introduced the bosonic annihilation and creation operators  $a = \sqrt{\frac{m\omega_o}{2\hbar}}(x + i\frac{p}{m\omega_o})$  and  $a^\dagger = \sqrt{\frac{m\omega_o}{2\hbar}}(x - i\frac{p}{m\omega_o})$ . The form of the Eq. (24) is similar to the Lindblad form master equation for the reduced density matrix of the system harmonic oscillator. The non-Markovian process is characterized by the time-dependent coefficients  $D_e(t)$  and  $\gamma_e(t)$  appearing in the master equation which is known as diffusion and dissipation coefficients, respectively. We assume that the NER system is initially prepared in one of the eigenstates of its Hamiltonian  $H_S$ , i.e., a Fock state  $|n\rangle$ . We are interested in the reduced system dynamics when its engineered artificial reservoir is switch off and on at a time interval  $\tau$ .<sup>45</sup> Consequently, each switching off and on process will reset the correlations between the system and environment. Assuming the initial oscillator state to be in a Fock state, the recursive use of the master equation [Eq. (24)] leads to the following equation for the density matrix of the reduced system (oscillator):<sup>15,44,45</sup>

$$\begin{aligned} \dot{\rho}_R(t) = & -\frac{i}{\hbar}[H_S, \rho_R(t)] \\ & + P_n^\downarrow(\tau) \left[ a\rho_R(t)a^\dagger - \frac{1}{2}a^\dagger a\rho_R(t) - \frac{1}{2}\rho_R(t)a^\dagger a \right] \\ & + P_n^\uparrow(\tau) \left[ a^\dagger \rho_R(t)a - \frac{1}{2}aa^\dagger \rho_R(t) - \frac{1}{2}\rho_R(t)aa^\dagger \right], \end{aligned} \quad (25)$$

where the decay coefficients are written as

$$P_n^\downarrow(\tau) = n \int_0^\tau [D_e(t) + \gamma_e(t)] d\tau \quad (26)$$

and

$$P_n^\uparrow(\tau) = (n+1) \int_0^\tau [D_e(t) - \gamma_e(t)] d\tau. \quad (27)$$

Here  $P_n^\downarrow(\tau)$  and  $P_n^\uparrow(\tau)$  are probabilities for the upward and downward transitions, respectively. For an initial Fock state  $|n\rangle$ , there exist two possible decay channels associated with the upward and downward transitions to the states  $|n+1\rangle$  and  $|n-1\rangle$ , respectively. The probability that the oscillator make a transition to the state  $|n-1\rangle$  or  $|n+1\rangle$  from its initial state  $|n\rangle$  after a short-time interval  $\tau$  can be written as  $\bar{P}_n(\tau) = P_n^\downarrow(\tau) + P_n^\uparrow(\tau)$ . Then the survival probability for the system to remain in its initial state  $P_n(\tau) = 1 - \bar{P}_n(\tau)$ . From Eq. (25), one gets

$$\frac{d\rho_{nn}(t)}{dt} = -\{(n+1)[D_e(t) - \gamma_e(t)] + n[D_e(t) + \gamma_e(t)]\}\rho_{nn}(t), \quad (28)$$

where  $\rho_{nn}(t) = \langle n | \rho_R(t) | n \rangle$  is the survival probability for the system to stay in the initial state  $|n\rangle$ . Frequent measurements at extremely short-time interval may slow down the decay process because the decay of the upward and downward states are almost zero at the beginning of the decay process.<sup>15,46</sup> The QZE predicts that the decay of the unstable system can be slowed down by measuring the system successively and frequently enough. A QZE typically arises if one performs a series of ‘‘measurements,’’ at a time interval  $\tau$ , in order to ascertain whether the system is still in its initial state.<sup>14</sup> For this measurement purpose, we use the term shuttered reservoir, and assume that  $\tau$  is so short that expansion yields a quadratic behavior. Let  $P_n(\tau)$  denotes the survival probability (after a short-time interval  $\tau$ ) for the system to stay at the initial state, which can be written as  $P_n(\tau) = \exp[-\gamma_n^Z(\tau)\tau]$ .<sup>46</sup> After the  $N$ th measurement the survival probability reads<sup>14,15,47</sup>

$$P_n^{(N)}(t) = P_n(\tau)^N \equiv \exp[-\gamma_n^Z(\tau)t], \quad (29)$$

where  $t = N\tau$  is the total duration of the experiment and  $\gamma_n^Z(\tau)$  is the effective decay rate.<sup>14</sup> In Eq. (29), we have assumed that the probability  $P_n(\tau)$  factorizes.<sup>14</sup> The behavior of the effective decay rate appearing in Eq. (29) also quantifies the Zeno or anti-Zeno effect. Assuming that  $\tau$  is small enough and keeping only the first two terms in the expansion of the exponential appearing in Eq. (29), one easily gets

$$\gamma_n^Z(\tau) = \frac{1}{\tau} \left[ (2n+1) \int_0^\tau D_e(t) d\tau - \int_0^\tau \gamma_e(t) d\tau \right]. \quad (30)$$

The quantification of the Zeno (QZE) and the anti-Zeno (AZE) effect is given by the ratio<sup>15</sup>

$$\frac{\gamma_n^Z(\tau)}{\gamma_n^0} = \frac{(2n+1) \int_0^\tau D_e(t) d\tau - \int_0^\tau \gamma_e(t) d\tau}{\tau[(2n+1)D_e^M - \gamma_e^M]}. \quad (31)$$

We indicate with  $\gamma_n^0$  the Markovian decay rate (the constant spectral density,  $\lambda \rightarrow \infty$ , and long-time limit) of the survival probability, as predicted by Fermi golden rule. If a finite time  $\tau^\dagger$  such that  $\gamma_n^Z(\tau^\dagger) = \gamma_n^0$  exists in the Markovian regime, then for  $\tau < \tau^\dagger$  we have  $\gamma_n^Z(\tau)/\gamma_n^0 < 1$ , i.e., the measurements hinder the decay (QZE). On the other hand, if it has  $\gamma_n^Z(\tau)/\gamma_n^0 > 1$ , and the measurements enhance the decay (AZE).<sup>15</sup> In the standard definition of the QZE, the behavior of the effective decay rate in Eq. (31) is associated with the Markovian rate,  $\gamma_n^0$ , identifies the occurrence of the Zeno or the anti-Zeno effect.<sup>15</sup> In contrast, we identify qualitative definition, the QZE takes place as the population decay rate decreases when  $\tau$  becomes smaller. On the other hand, when the decay rate increases for smaller  $\tau$ , i.e., measurements enhance the decay, shows the AZE.<sup>47</sup>

$D_e^M$  and  $\gamma_e^M$  describes Markovian values of the diffusion and damping coefficients, respectively. If a finite time  $\tau^\dagger$  such that  $\gamma_n^Z(\tau^\dagger) = \gamma_n^0$  exists in the Markovian region, then for  $\tau < \tau^\dagger$ , we have  $\gamma_n^Z(\tau)/\gamma_n^0 < 1$ , i.e., the measurements hinder the decay (QZE). On the other hand, we have  $\gamma_n^Z(\tau)/\gamma_n^0 > 1$ , i.e., the measurements enhance the decay (AZE). The analytic expression of the diffusion (damping) coefficients allows us to work out the relevant system and reservoir parameters showing the crossover between the QZE and AZE in Eq. (31). The Markovian dynamics of the nanomechanical resonator is recovered at large-time limit of the non-Markovian counterpart. Here we investigate the occurrence of either QZE or AZE of a nanomechanical oscillator coupled to a nonequilibrium fermionic reservoir (quantum point-contact detector acting as a measuring device). The QPC, considered here, is a charge-sensitive detector that can be easily controlled by the source and drain electric bias and bath temperature. The eigenstates of the oscillator are not localized, either in position or in momentum, and it is sensitive to the environment-induced dissipation. Figure 3 displays the effective decay rate over a shuttering time period of the frequent observations. It illustrates how a nanomechanical oscillator coupled to a nonequilibrium fermionic reservoir (a QPC acting as measuring device) exhibits the Zeno and the anti-Zeno effect. Moreover, one can control the shuttering time of effective environment by doing switch on-off the electric bath of finite temperature and finite bias voltage across QPC. In Figs. 3(a<sub>1</sub>)–3(c<sub>1</sub>), we plot the ratio between the effective decay rate  $\gamma_n^Z(\tau)$  and the Markovian decay rate  $\gamma_n^0$  from the high to the low cutoff regime for electric bath of different temperature strengths. Figures 3(a<sub>2</sub>)–3(c<sub>2</sub>) show the variation in the ratio of the diffusion coefficient  $D_e(\tau)$  and its Markovian value  $D_M$  from the high to the low cutoff regime for electric bath of different temperature strengths. Our analysis shows that there exist two relevant parameters, namely, the ratio  $\lambda/\omega_0$ , quantifying the spectral cutoff strength, and the ratio  $k_B T/\omega_0$ . We find that for high temperature,  $\beta=0.1\omega_0$ , a Zeno-type situation exists from high to low cutoff strengths as it is shown in Figs. 3(a<sub>1</sub>)–3(c<sub>1</sub>). This can

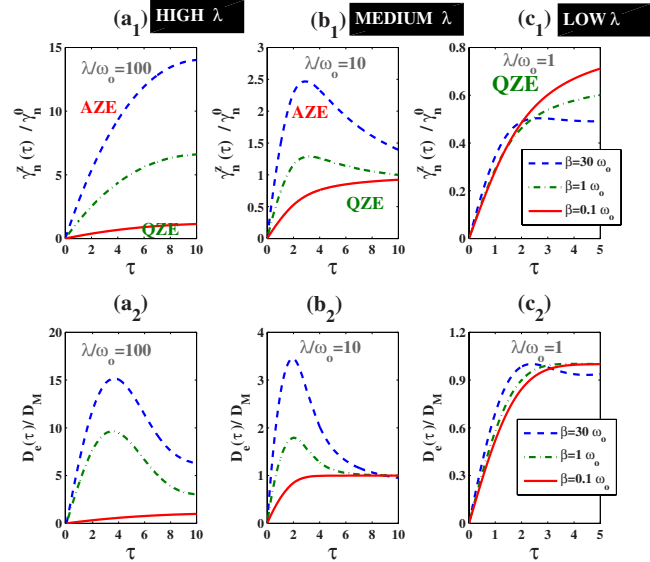


FIG. 3. (Color online) (a<sub>1</sub>) Ratio between the effective decay rate  $\gamma_n^Z(\tau)$  and the Markovian decay rate  $\gamma_n^0$  are plotted in the high cutoff ( $\lambda=100\omega_0$ ) regime for electric bath of different temperature strengths. (a<sub>2</sub>) Ratio of the diffusion coefficient  $D_e(\tau)$  and its Markovian value  $D_M$  are plotted in the high cutoff regime for electric bath of different temperature strengths. (b<sub>1</sub>) Ratio between the effective decay rate  $\gamma_n^Z(\tau)$  and the Markovian decay rate  $\gamma_n^0$  are plotted in intermediate cutoff regime for electric bath of different temperature strengths. (b<sub>2</sub>) Ratio of the diffusion coefficient  $D_e(\tau)$  and its Markovian value  $D_M$  are shown in the intermediate cutoff regime for electric bath of different temperature strengths. (c<sub>1</sub>) Ratio between the effective decay rate  $\gamma_n^Z(\tau)$  and the Markovian decay rate  $\gamma_n^0$  are shown in low cutoff regime for electric bath of different temperature strengths. (c<sub>2</sub>) Ratio of the diffusion coefficient  $D_e(\tau)$  and its Markovian value  $D_M$  are plotted in low cutoff regime for electric bath of different temperature strengths. The value of the other parameters are  $eV=0.1\omega_0$ ;  $\beta=30$ .

be understood due to environment-induced decoherence by showing the short-time dynamics of  $D_e(\tau)/D_M$ . For high reservoir temperatures, the quantity effectively ruling the dynamics is the diffusion coefficient  $D_e(t)$  since  $D_e(t) \gg \gamma_e(t)$ . In other words, for short times and high temperature, the diffusion,  $D_e(t)$  is dominant with respect to dissipation. For decreasing temperatures, the amplitudes of  $D_e(t)$  becomes smaller. For very low reservoir temperatures ( $k_B T \approx 0, n \approx 0$ ),  $D_M \approx \gamma_M$  and therefore the denominator of Eq. (31) approaches zero, implying that  $\gamma_n^Z(\tau)/\gamma_n^0 \gg 1$  where measurement enhance the decay (AZE) for short evolution time. Generally in the study of a nanomechanical oscillator coupled to a nonequilibrium fermionic reservoir (a QPC acting as measuring device), one assumes high cutoff strength ( $\lambda/\omega_0=100$ ) corresponding to a natural Markovian reservoir with  $\lambda \rightarrow \infty$ . In this case, it is straightforward to show that  $D_e(t) \gg \gamma_e(t)$  for short evolution times. When the expectation values of diffusion term is greater than its Markovian value, the measured system goes through a stronger effective environment-induced decoherence resulting to a faster or accelerated decay (AZE) of the system as shown in Fig. 3 in

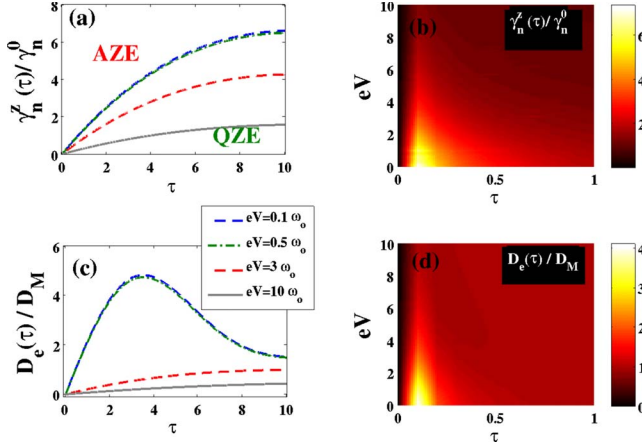


FIG. 4. (Color online) (a) Ratio between the effective decay rate  $\gamma_n^Z(\tau)$  and the Markovian decay rate  $\gamma_n^0$  are plotted in the high cutoff regime for electric bias-voltage strengths ( $eV/\omega_o=0.1, 0.5, 3, 10$ ). (c) Ratio of the diffusion coefficient  $D_e(\tau)$  and its Markovian value  $D_M$  are shown in the high cutoff regime for different electric bias-voltage strengths ( $eV/\omega_o=0.1, 0.5, 3, 10$ ). The value of the other parameters in (a) and (c) are  $\lambda=100\omega_o$ ,  $\beta=30\omega_o$ . (b) Function of the bias voltage with ratio between the effective decay rate  $\gamma_n^Z(\tau)$  and the Markovian decay rate  $\gamma_n^0$  are plotted contour in the high cutoff regime for different electric bias-voltage strengths. (d) Function of the bias voltage with ratio of the diffusion coefficient  $D_e(\tau)$  and its Markovian value  $D_M$  are shown in the high cutoff regime for different electric bias-voltage strengths. The value of the other parameters in (b) and (d) are  $\lambda=100\omega_o$  and  $\beta=30\omega_o$ .

low temperature and higher cutoff strength. On the contrary, when the effect of environment-induced decoherence is smaller than Markovian one, the QZE occurs as shown in Fig. 3 in the high temperature and higher cutoff strength.

To better understand such a behavior of exhibiting Zeno and anti-Zeno effects, we consider three different regimes of the ratio  $\lambda/\omega_o$  between the reservoir cutoff frequency and the system oscillator frequency: high cutoff  $\lambda/\omega_o=100$ , intermediate cutoff  $\lambda/\omega_o=10$ , and low cutoff  $\lambda/\omega_o=1$  regimes. From Figs. 4(a), 5(a), and 6(a) we see that for high voltage ( $eV=10\omega_o$ ), a Zeno-type situation exists for any arbitrary value of the cutoff strengths. For high electric bias voltage, the quantity effectively ruling the dynamics is the diffusion coefficient  $D_e(t)$  since  $D_e(t) \gg \gamma_e(t)$ . In this case, the effective decay rate depends only on the diffusion coefficient  $D_e(t)$ . In other words, for short times and high electric bias voltage, the diffusion is mainly dominant with respect to dissipation. The reason is a strong environment-induced decoherence, for which the effect of environment-induced decoherence is smaller than Markovian one, the QZE occurs.

On the other hand, for decreasing electric bias voltage, the amplitudes of  $D_e(t)$  becomes smaller for a smaller environment-induced decoherence. For a reservoir with very low electric bias voltage ( $eV \ll \omega_o$ ),  $D_M \approx \gamma_M$  and the denominator of Eq. (31) approaches zero, implying that  $\gamma_n^Z(\tau)/\gamma_n^0 \gg 1$  where the measurement enhance the decay. It shows that a Zeno-anti-Zeno crossover appears with anti-Zeno effect appearing for short evolution time, and Zeno effect appearing for long times. This can be observed as a crossing between Zeno to anti-Zeno region as shown in Figs.

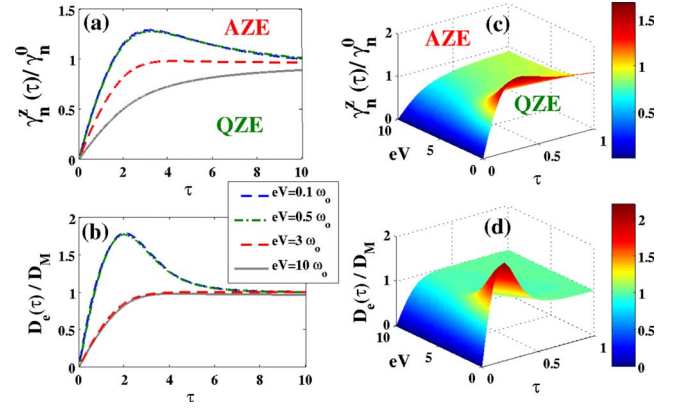


FIG. 5. (Color online) (a) Ratio between the effective decay rate  $\gamma_n^Z(\tau)$  and the Markovian decay rate  $\gamma_n^0$  are plotted in the intermediate cutoff regime for different electric bias-voltage strengths. (c) Ratio of the diffusion coefficient  $D_e(\tau)$  and its Markovian value  $D_M$  are shown in the intermediate cutoff regime for different electric bias-voltage strengths. The value of the other parameters in (a) and (c) are  $\lambda=10\omega_o$ ,  $\beta=30\omega_o$ . (b) Function of the bias voltage with ratio between the effective decay rate  $\gamma_n^Z(\tau)$  and the Markovian decay rate  $\gamma_n^0$  are plotted three-dimensional in the intermediate cutoff regime for different electric bias-voltage strengths. (d) Function of the bias voltage with ratio of the diffusion coefficient  $D_e(\tau)$  and its Markovian value  $D_M$  are shown in the intermediate cutoff regime for different electric bias-voltage strengths. The value of the other parameters in (b) and (d) are  $\lambda=10\omega_o$  and  $\beta=30\omega_o$ .

4(b) and 5(b). In the low cutoff frequency regimes, it corresponds to an engineered “out-of-resonance” reservoir.<sup>13</sup> In this case, the reservoir correlation time is bigger than the nanomechanical oscillator period. Another interesting aspect is the in intermediate cutoff regime, where it is shown (Fig. 5) that a Zeno-anti-Zeno crossover exists for smaller electronic bias or low temperature. For  $\omega_o \sim \lambda$ , the region in which only Zeno dynamics may occur in low cutoff energy due to smaller decoherence is shown in Fig. 6.

#### IV. CONCLUSION

In summary, we have presented and discussed the influence of the fermionic reservoir on the occurrence of QZE or AZE by varying finite cutoff frequency, electric bias-voltage strengths, and the electric bath temperature. We have investigated the non-Markovian dynamics of nanomechanical oscillator coupled to a nonequilibrium fermionic reservoir, implemented with the memory kernel prescription, by partially taking trace over the detector’s microscopic degrees of freedom. We stress that the Markovian approximation is not applicable when the characteristic time of the relevant system become comparable with the reservoir correlation time showing the memory effect of the environment. By regarding the tunneling Hamiltonian as perturbation, the second-order cumulant expansion (Born approximation) leads to the master equation for the reduced density matrix of the central transport system. We derived non-Markovian form of the master equation, implemented with the memory kernel prescription, by partially taking trace over the detector’s micro-

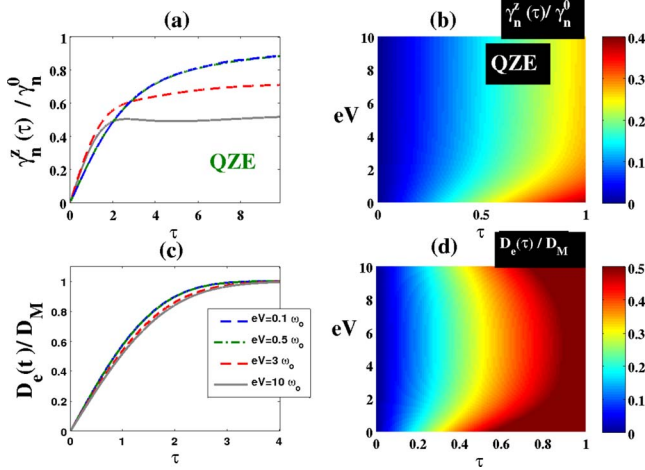


FIG. 6. (Color online) (a) Ratio between the effective decay rate  $\gamma_n^e(\tau)$  and the Markovian decay rate  $\gamma_n^0$  are plotted in the low cutoff regime for different electric bias-voltage strengths. (c) Ratio of the diffusion coefficient  $D_e(\tau)$  and its Markovian value  $D_M$  are shown in the low cutoff regime for different electric bias-voltage strengths. The parameters are  $\beta=30\omega_0$ ;  $\lambda=1$ , up line down line with  $eV=0.1, 0.5, 3, 10\omega_0$  shown that (a) and (c) parts. (b) Function of the bias voltage with ratio between the effective decay rate  $\gamma_n^e(\tau)$  and the Markovian decay rate  $\gamma_n^0$  are plotted contour in the low cutoff regime for different electric bias-voltage strengths. (d) Function of the bias voltage with ratio of the diffusion coefficient  $D_e(\tau)$  and its Markovian value  $D_M$  are shown in the low cutoff regime for different electric bias-voltage strengths. Other parameters are used  $\lambda=1$ ,  $\beta=30\omega_0$  shown that (b) and (d) parts.

scopic degree of freedom. In the Markovian limit, the master equation is of the form of Caldeira-Leggett type, consists of a damping and decoherence terms, even though the electronic environment is in a nonequilibrium state. We report our numerical results of these coefficients depending uniquely on the form of the reservoir spectral density, environmental temperature, and bias voltage in the non-Markovian regime.

We have investigated the occurrence of either QZE or AZE of a nanomechanical oscillator coupled to a nonequilibrium fermionic reservoir (quantum point-contact detector acting as a measuring device). The transition from Zeno to anti-Zeno behavior can be controlled by changing the values of the system and reservoir parameters (such as the oscillator frequency, energy cutoff, bias voltage, and reservoir temperature).

#### ACKNOWLEDGMENTS

We would like to acknowledge support from the Excellent Research Projects of the National Taiwan University under Grant No. 97R0066-65, and we thank Hsi-Sheng Goan for useful comments and discussion.

#### APPENDIX

In this section, we show that under appropriate limits, our non-Markovian master equation reduces to the Markovian

master equation as reported in the literature.<sup>25–27</sup> The Markovian approximation is known to be valid when the bath correlation time is much smaller than the characteristic time scale of the system of interest. The environment correlation time is determined by the bath correlation functions (kernels) and is associated with the form of spectral density. Under the Markovian limit, the bath correlation function (kernel) is  $\delta$  correlated in time and integration limit  $t$  in Eqs. (13)–(16) for QPC reservoirs can be taken as  $t \rightarrow \infty$ . Thus, if we take the Markovian approximation of very short correlation times (integration limit  $t \rightarrow \infty$ ) and the wideband limit ( $\lambda \rightarrow \infty$ ), then the time-dependent coefficients in the master Eqs. (8), (12), and (17) become time independent. On making use of the formula

$$\lim_{t \rightarrow \infty} \int_0^t d\tau e^{i(\omega - \omega_0)\tau} = \pi \delta(\omega - \omega_0) + iPV\left(\frac{1}{\omega - \omega_0}\right), \quad (\text{A1})$$

where  $PV$  indicates the Cauchy principle value. The functions in Eqs. (13)–(16) for QPC reservoirs can be written as

$$\lim_{t \rightarrow \infty} f_{F(B)}^\pm(t, x) \equiv W(x) \pm i\Theta_{F(B)}(x), \quad (\text{A2})$$

where

$$W(x) = \pi \frac{x}{1 - e^{-x/k_B T}}, \quad (\text{A3})$$

$$\begin{aligned} \Theta_{F(B)}(x) &= \int_{-\infty}^{\infty} \int_{-\infty}^{\infty} d\omega_k^S d\omega_q^D \frac{J_{W,Z}(\epsilon_k^S, \epsilon_q^D)}{W_{00} Z_{00}} \\ &\times \frac{1}{e^{\beta\omega_k^S} + 1} \left(1 - \frac{1}{e^{\beta\omega_q^D} + 1}\right) PV\left(\frac{1}{\omega_k^S - \omega_q^D - x}\right), \end{aligned} \quad (\text{A4})$$

$$\begin{aligned} \Theta_{B(F)}(x) &= \int_{-\infty}^{\infty} \int_{-\infty}^{\infty} d\omega_k^S d\omega_q^D \frac{J_{W,Z}(\epsilon_k^S, \epsilon_q^D)}{W_{00} Z_{00}} \\ &\times \frac{1}{e^{\beta\omega_q^D} + 1} \left(1 - \frac{1}{e^{\beta\omega_k^S} + 1}\right) PV\left(\frac{1}{\omega_k^S - \omega_q^D - x}\right). \end{aligned} \quad (\text{A5})$$

The real part  $W(x) = \frac{x}{1 - \exp[-\beta x]}$  describes the tunneling rate and the imaginary part  $\Theta_{F(B)}(x)$  is Cauchy principal value. Using Eq. (A2) in Eq. (17), we can have the Markovian Master equation,<sup>27</sup>

$$\begin{aligned} \dot{\rho}_R &= \frac{1}{i\hbar} [H_S, \rho_R] - \frac{i}{\hbar} \gamma_e^M [x, \{p, \rho_R\}] - \frac{1}{\hbar^2} D_e^M [x, [x, \rho_R]] \\ &+ \frac{1}{\hbar^2} h_e^M [x, [p, \rho_R]], \end{aligned} \quad (\text{A6})$$

where the bare oscillator Hamiltonian,  $H_S = \frac{1}{2} M \omega_0^2 x^2$ , comes from the antisymmetric combinations of the distribution function in Eq. (10). It can be seen that at large times, the frequency shift,  $\omega_e^2(t)$ , is equal to  $-\omega_e^2$ . The added counter-term is to cancel the frequency shift at long times and the system cannot lower its potential energy below the original

(bare oscillator frequency to the oscillator frequency with the renormalized, the shift is compensated to counterterm value.<sup>9,27</sup>

As a result, in the Markovian limit, the frequency renormalization, the damping coefficient, and the diffusion coefficients in Eqs. (18)–(21) due to the QPC reservoirs in the wideband limit ( $\lambda \rightarrow \infty$ ) become, respectively,

$$(\omega_e^M)^2 = \frac{\alpha}{\pi M} \{ \Theta_F[eV + \hbar\omega_o] - \Theta_B[-eV - \hbar\omega_o] + \Theta_F[eV - \hbar\omega_o] - \Theta_B[-eV + \hbar\omega_o] \}, \quad (\text{A7})$$

$$\gamma_e^M = \frac{\hbar}{M} \alpha, \quad (\text{A8})$$

$$D_e^M = \frac{\hbar\alpha}{2} \left[ (eV + \hbar\omega_o) \coth \frac{eV + \hbar\omega_o}{2k_B T} + (eV - \hbar\omega_o) \coth \frac{eV - \hbar\omega_o}{2k_B T} \right], \quad (\text{A9})$$

$$h_e^M = \frac{\hbar\alpha}{2\pi M\omega_o} \{ \Theta_F[eV + \hbar\omega_o] + \Theta_B[-eV - \hbar\omega_o] - \Theta_F[eV - \hbar\omega_o] - \Theta_B[-eV + \hbar\omega_o] \}. \quad (\text{A10})$$

We recall that the dissipation and the noise kernel  $D_e^M$  and  $\gamma_e^M$  were introduced in the Eqs. (A8) and (A9). The Markovian limit is obtained in the  $t \rightarrow \infty$  and wideband (WB) limit. Then it originates,  $h_e^M$ , in symmetric combinations of the distribution function [Eq. (9)] via integrals of Fermi surface that is energy shift or virtual processes in Eq. (A10).<sup>27</sup> In Eq. (A6), time-independent coefficients are exact solution with the previous paper<sup>27</sup> that is taking trace over the detector's microscopic degree of freedom.

\*powen@phys.ntu.edu.tw

<sup>1</sup>Q. A. Turchette, C. J. Myatt, B. E. King, C. A. Sackett, D. Kielpinski, W. M. Itano, C. Monroe, and D. J. Wineland, *Phys. Rev. A* **62**, 053807 (2000).

<sup>2</sup>I. Bloch, *Nat. Phys.* **1**, 23 (2005).

<sup>3</sup>R. G. Knobel and A. N. Cleland, *Nature (London)* **424**, 291 (2003).

<sup>4</sup>M. LaHaye, O. Buu, B. Camarota, and K. C. Schwab, *Science* **304**, 74 (2004).

<sup>5</sup>D. Mozyrsky, I. Martin, and M. B. Hastings, *Phys. Rev. Lett.* **92**, 018303 (2004).

<sup>6</sup>X. M. Henry Huang, C. A. Zorman, M. Mehregany, and M. L. Roukes, *Nature (London)* **421**, 496 (2003).

<sup>7</sup>A. Cho, *Science* **299**, 36 (2003); A. D. Armour, M. P. Blencowe, and K. C. Schwab, *Phys. Rev. Lett.* **88**, 148301 (2002).

<sup>8</sup>M. R. Geller and A. N. Cleland, *Phys. Rev. A* **71**, 032311 (2005); A. N. Cleland and M. R. Geller, *Phys. Rev. Lett.* **93**, 070501 (2004).

<sup>9</sup>H. P. Breuer and F. Petruccione, *The Theory of Open Quantum Systems* (Oxford University Press, Oxford, 2002).

<sup>10</sup>D. Giulini, E. Joos, C. Kiefer, J. Kupsch, and I. O. Stamatescu, *Decoherence and Appearance of a Classical World in Quantum Theory* (Springer, Berlin, 1996).

<sup>11</sup>V. B. Braginsky and F. Y. Khalili, *Quantum Measurement* (Cambridge University Press, Cambridge, 1992).

<sup>12</sup>C. W. Gardiner and P. Zoller, *Quantum Noise*, 2nd ed. (Springer-Verlag, Berlin, 2000).

<sup>13</sup>S. Maniscalco, J. Piilo, F. Intravaia, F. Petruccione, and A. Messina, *Phys. Rev. A* **70**, 032113 (2004).

<sup>14</sup>P. Facchi, H. Nakazato, and S. Pascazio, *Phys. Rev. Lett.* **86**, 2699 (2001).

<sup>15</sup>S. Maniscalco, J. Piilo, and K. A. Suominen, *Phys. Rev. Lett.* **97**, 130402 (2006).

<sup>16</sup>H. Park, J. Park, A. K. L. Lim, E. H. Anderson, A. P. Alivisatos, and P. L. McEuen, *Nature (London)* **407**, 57 (2000).

<sup>17</sup>C. J. Myatt, B. E. King, Q. A. Turchette, C. A. Sackett,

D. Kielpinski, W. M. Itano, C. Monroe, and D. J. Wineland, *Nature (London)* **403**, 269 (2000).

<sup>18</sup>S. Maniscalco, J. Piilo, F. Intravaia, F. Petruccione, and A. Messina, *Phys. Rev. A* **69**, 052101 (2004).

<sup>19</sup>M. W. Y. Tu and W. M. Zhang, *Phys. Rev. B* **78**, 235311 (2008).

<sup>20</sup>N. S. Wingreen and Y. Meir, *Phys. Rev. B* **49**, 11040 (1994).

<sup>21</sup>S. Welack, M. Schreiber, and U. Kleinekathofer, *J. Chem. Phys.* **124**, 044712 (2006).

<sup>22</sup>U. Kleinekathofer, *J. Chem. Phys.* **121**, 2505 (2004).

<sup>23</sup>T. S. Ho, S. H. Hung, H. T. Chen, and Shih-I Chu, *Phys. Rev. B* **79**, 235323 (2009).

<sup>24</sup>S. Datta, *Electronic Transport in Mesoscopic System* (Cambridge University Press, Cambridge, 1995); Y. Imry, *Introduction to Mesoscopic Physics* (Oxford University Press, New York, 1997).

<sup>25</sup>D. Mozyrsky and I. Martin, *Phys. Rev. Lett.* **89**, 018301 (2002).

<sup>26</sup>A. A. Clerk and S. M. Girvin, *Phys. Rev. B* **70**, 121303(R) (2004).

<sup>27</sup>J. Wabnig, D. V. Khomitsky, J. Rammer, and A. L. Shelankov, *Phys. Rev. B* **72**, 165347 (2005).

<sup>28</sup>A. Y. Smirnov, L. G. Mourkh, and N. J. M. Horing, *Phys. Rev. B* **67**, 115312 (2003).

<sup>29</sup>J. Wabnig, J. Rammer, and A. L. Shelankov, *Phys. Rev. B* **75**, 205319 (2007).

<sup>30</sup>H. J. Carmichael, *Statistical Methods in Quantum Optics I* (Springer, Berlin, 1999).

<sup>31</sup>T. M. Stace and S. D. Barrett, *Phys. Rev. Lett.* **92**, 136802 (2004).

<sup>32</sup>J. P. Paz and W. H. Zurek, in *Coherent Matter Waves*, Proceedings of the Les Houches Summer School, Vol. LXXII, edited by R. Kaiser, C. Westbrook, and F. David (Springer-Verlag, Berlin, 2001).

<sup>33</sup>X. Q. Li, W. K. Zhang, P. Cui, J. Shao, Z. Ma, and Y. J. Yan, *Phys. Rev. B* **69**, 085315 (2004).

<sup>34</sup>X. Q. Li, P. Cui, and Y. J. Yan, *Phys. Rev. Lett.* **94**, 066803 (2005).

<sup>35</sup>M. T. Lee and W. M. Zhang, *J. Chem. Phys.* **129**, 224106

- (2008).
- <sup>36</sup>C. Meier and D. J. Tannor, *J. Chem. Phys.* **111**, 3365 (1999).
- <sup>37</sup>The spectral density specifies the structure and properties of the environment and determines the environmental influence on the dynamics of the system of interest. In principle, we could deal with any energy-dependent densities of state and tunneling amplitudes to take into account the memory effect of the QPC reservoir in our non-Markovian treatment. For simplicity, we follow several non-Markovian electron-transport studies (Refs. 19–21 and 35) by considering a spectral density with energy-dependent densities of states and tunneling amplitudes approximately treated as a Lorentzian form.
- <sup>38</sup>W. T. Strunz and T. Yu, *Phys. Rev. A* **69**, 052115 (2004).
- <sup>39</sup>B. L. Hu, J. P. Paz, and Y. Zhang, *Phys. Rev. D* **45**, 2843 (1992).
- <sup>40</sup>D. A. Rodrigues and A. D. Armour, *New J. Phys.* **7**, 251 (2005).
- <sup>41</sup>Our architecture is similar to that of Ref. 27 in Eq. (A7), it explores the coupled to environment inducing a frequency shift. Starting from the original Hamiltonian from *bare* frequency since the coupling to environment (Ref. 9) in page 465–466, where  $\omega_b^2$  is the bare frequency in the system Hamiltonian. The coefficient  $\omega_e^2(t)$  is leading to time-dependent energy shift due to quantum point contact (Fermi reservoir). The bare frequency is connected to the renormalized frequency  $\omega_o$  by the relation,  $\omega_b^2 = \omega_0^2 + \omega_c^2$ . Then the physical frequency in this case is  $\omega_p^2(t) = \omega_b^2 + \omega_e^2(t)$ ,  $\omega_c^2$  and  $\omega_e^2(t)$  tend to compensate each other in the long-time limit, such that the observable frequency  $\omega_p^2(t)$  is close to the renormalized frequency  $\omega_0$ .
- <sup>42</sup>A. O. Caldeira and A. J. Leggett, *Physica* **121A**, 587 (1983); *Ann. Phys. (N.Y.)* **149**, 374 (1983).
- <sup>43</sup>R. Karrlein and H. Grabert, *Phys. Rev. E* **55**, 153 (1997).
- <sup>44</sup>F. Intravaia, S. Maniscalco, and A. Messina, *Phys. Rev. A* **67**, 042108 (2003).
- <sup>45</sup>D. Maor, P. J. Cooney, A. Faibis, E. P. Kanter, W. Koenig, and B. J. Zabransky, *Phys. Rev. A* **32**, 105 (1985).
- <sup>46</sup>H. Zheng, S. Y. Zhu, and M. S. Zubairy, *Phys. Rev. Lett.* **101**, 200404 (2008).
- <sup>47</sup>D. Segal and D. R. Reichman, *Phys. Rev. A* **76**, 012109 (2007).